ELSEVIER

Journal of Applied Geophysics 32 (1994) 85–98

APPLIED GEOPHYSICS

A large scale geophysical survey in the archaeological site of Europos (northern Greece)

G.N. Tsokas[a], A. Giannopoulos[b], P. Tsourlos[b], G. Vargemezis[a], J.M. Tealby[b], A. Sarris[c], C.B. Papazachos[a], T. Savopoulou[d]

[a]*Geophysical Laboratory, Aristotle University of Thessaloniki, 54006 Thessaloniki, Macedonia, Greece*
[b]*Department of Electronics, University of York, Heslington, York, YO1 5DD, UK*
[c]*Department of Physics and Astronomy, Behlen Laboratory of Physics, Linkon, NE 68588-0111, USA*
[d]*Archaeological Museum of Thessaloniki, H.A.N.Th. Square, Thessaloniki, Macedonia, Greece*

(Received February 18, 1993; accepted after revision October 12, 1993)

Abstract

The results of a large scale exploration of an archaeological site by geophysical means are presented and discussed. The operation took place in the site where the ruins of the ancient city of Europos are buried. This site is in northern Greece.

Resistivity prospecting was employed to detect the remnants of wall foundations in the place where the main urban complex of the ancient city once stood. The data were transformed in an image form depicting, thus, the spatial variation of resistivity in a manner that resembles the plane view of the ruins that could have been drawn if an excavation had taken place.

This image revealed the urban plan of the latest times of the life of the city. Trial excavations verified the geophysical result. Magnetic prospecting in the same area complemented the resistivity data. The exact location of the fire hearths, kilns and remnants of collapsed roofs were spotted.

Magnetic gradient measurements were taken in an area out of the main complex of the ancient city and revealed the location of several kilns. One of these locations was excavated and a pottery kiln was discovered.

The resistivity prospecting in one of the graveyards of the ancient city showed anomalies which were expected and corresponded to monumental tombs. The locations of a few of them were excavated and large burial structures were revealed.

Ground probing radar profiles were measured over the tombs which showed pronounced resistivity anomalies, so far unearthed. The relatively high resolving ability of the method assisted the interpretation in the sense that a few attributes were added. In the presented case, it was concluded that a particular tomb consists of two rooms and that it is roofless.

1. Introduction

The geophysical exploration of archaeological sites became a common practice a long time ago. The tendency of the last decade was to cover large areas, i.e. to acquire data as complete as possible with respect to a particular archaeological site. After processing, the results had to be presented in some form that could be read by non-experts (Scollar et al., 1986; Wynn, 1986). Therefore, techniques were developed which transform the geophysical results into an image that resembles the plane view of the buried relics, i.e. the result that could have been drawn if an excavation had taken place.

The large scale survey presented in the following pages was conducted in the site where the ruins of an ancient city named Europos are hosted. It was a multipurpose survey, aiming to explore not only the area

SSDI 0926-9851 (93) E0039-C

which is presumably within the city walls but also all the areas used by the ancient inhabitants. At first we tried to reveal the urban street network. We then detected the workshops of craftsmen (like pottery kilns) in the surrounding area. The location of monumental tombs in various cemeteries of the ancient city comprised other major aims of the survey.

The location of the site shown in Fig. 1 is in the northern Greek territory, which is in the region of Macedonia, close to the banks of Axios river. Palaeogeographical studies in the area (Astaras and Sotiriadis, 1988) have shown that the sea was much closer to the ancient city than it is today. This corresponds with the ancient literature sources which claim that the ancient city was a commercial centre due to its harbour on the river Axios. It seems that the ships used to sail a small distance against the flow of the river and deliver their cargoes at the port of Europos.

The lay out of the survey is shown in Fig. 2. The various locations which belong to the ensemble of the ancient city have been marked on the figure by a code. The main urban complex of the ancient city lies in the place marked as *AKR* and was explored by magnetic and resistivity means. The code *EUP* denotes the area where the workshops of the ancient city were located.

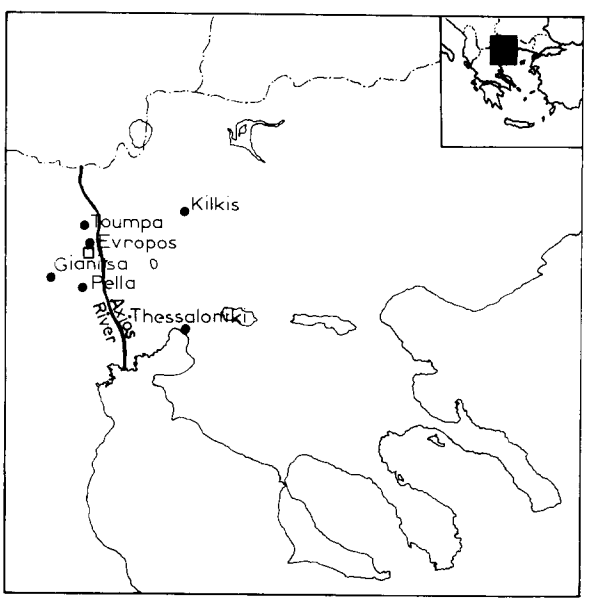

Fig. 1. The location of the site which hosts the ruins of the ancient commercial centre Europos in northern Greece is annotated with an open square. The modern village bears the same name and borders the archaeological site.

Magnetic field gradient measurements were employed for this case because the targets were expected to be mainly kilns. The kilns were made by baked clay and thus they exhibit pronounced magnetic effects. This location is in a lowered area with respect to the one marked as *AKR*. The codes *EURCEM* and *EURES* denote both the locations which were used as cemetery during Roman times. The limits of several trial pits dug in the area have been drawn in the figure by solid lines. The ruins which revealed by these excavations have been also drawn in their respective locations in the pits.

2. Exploration in the location of the ancient Acropolis

The area of the ancient "Acropolis" is marked with the code *AKR* in Fig. 2. The term Acropolis is used to denote the area of an ancient city, protected by walls and usually standing on an elevated location. In the present case the Acropolis is on top of a hill overlooking the Axios river basin.

2.1 Magnetic survey

Magnetic prospecting took place in the area of Fig. 2 which is enclosed by the bold solid line. Solid lines outline the group of 20×20 m^2 squares established in the particular location to carry out the measurements. The survey progressed by adding new 20×20 m^2 squares every day of work. The initial squares (numbers 1–6 in Fig. 2) were established on the ground surface using staff and levels. The others were built on the existing squares using simply two measuring tapes and taking advantage of the rule of squares for orthogonal triangles. In each 20×20 m^2 square, the magnetic field was recorded stepwise at 1 m intervals along traverses spaced 1 m apart from each other, using a *SCINTREX* proton-magnetometer. A second instrument was installed at a base station and its records were used to reduce the Earth's magnetic field daily variation from the data. That instrument was set so to register one reading per minute. Due to the manner of this correction, some noise appeared as a systematic rising or lowering of the measurements along specific profiles, during days which presumably had a moderate geomagnetic activity (Weymouth and Lessard, 1986). This noise is attributed to geomagnetic field distur-

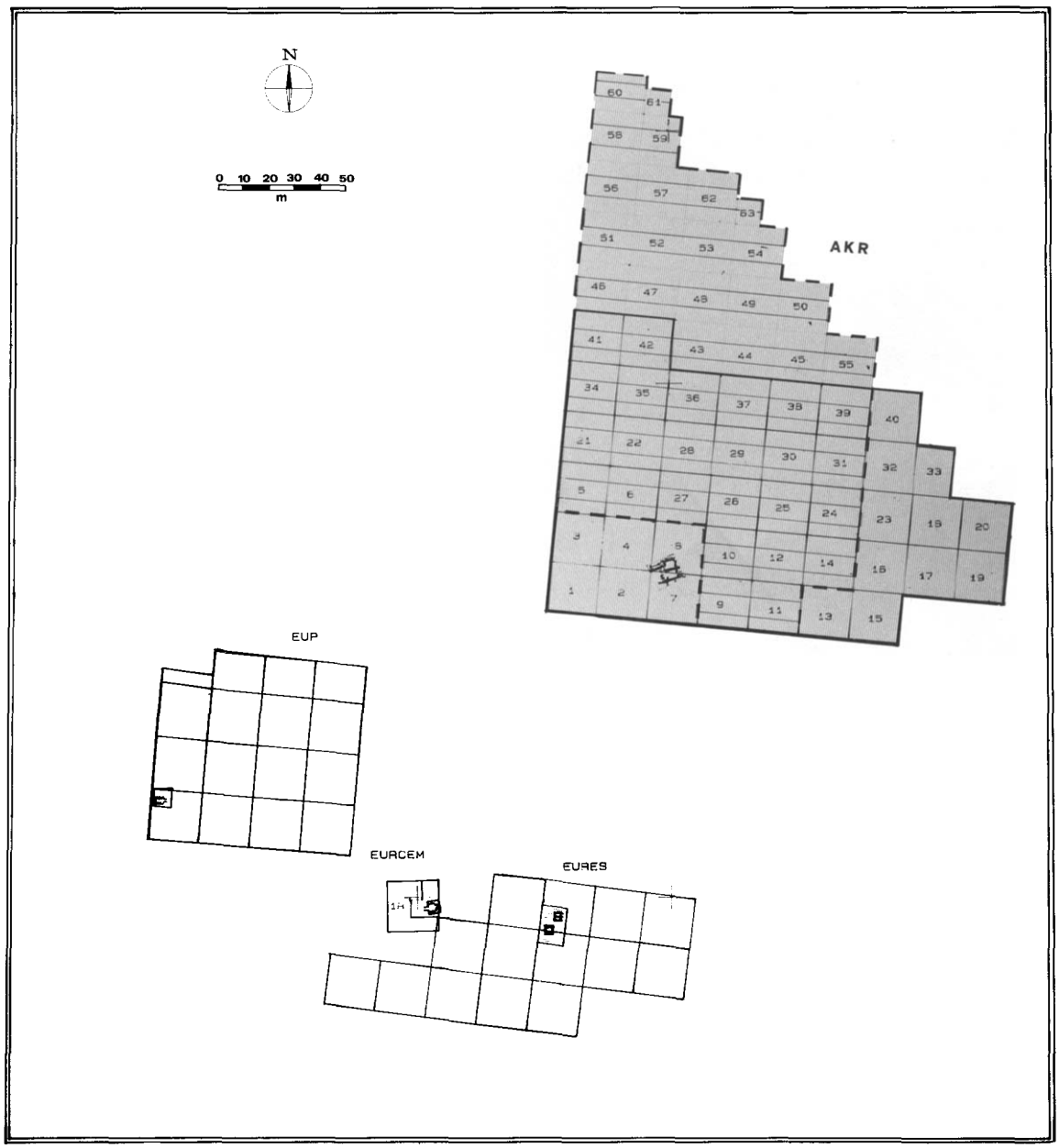

Fig. 2. Lay out of the measuring grids in the archaeological site of Europos. Various locations used for different purposes in the past have been annotated by a code. The code *AKR* stands for Acropolis, *EUP* for the location of the workshops while *EURCEM/EURES* mark the location of the cemetery of Roman times. Several excavation pits dug in the area have been drawn along with the plane view of the revealed ruins. The pits were suggested by the interpretation of geophysical maps.

bances with less than the period of a minute. The corresponding profiles were levelled by the subtraction of a factor which was determined as the difference of the profile mean value from the mean value along the two neighbouring ones (Sarris, 1992). After the referred correction, a linear trend was removed from the data.

The data were then subjected to despiking and smoothing. The term "despiking" covers two opera-

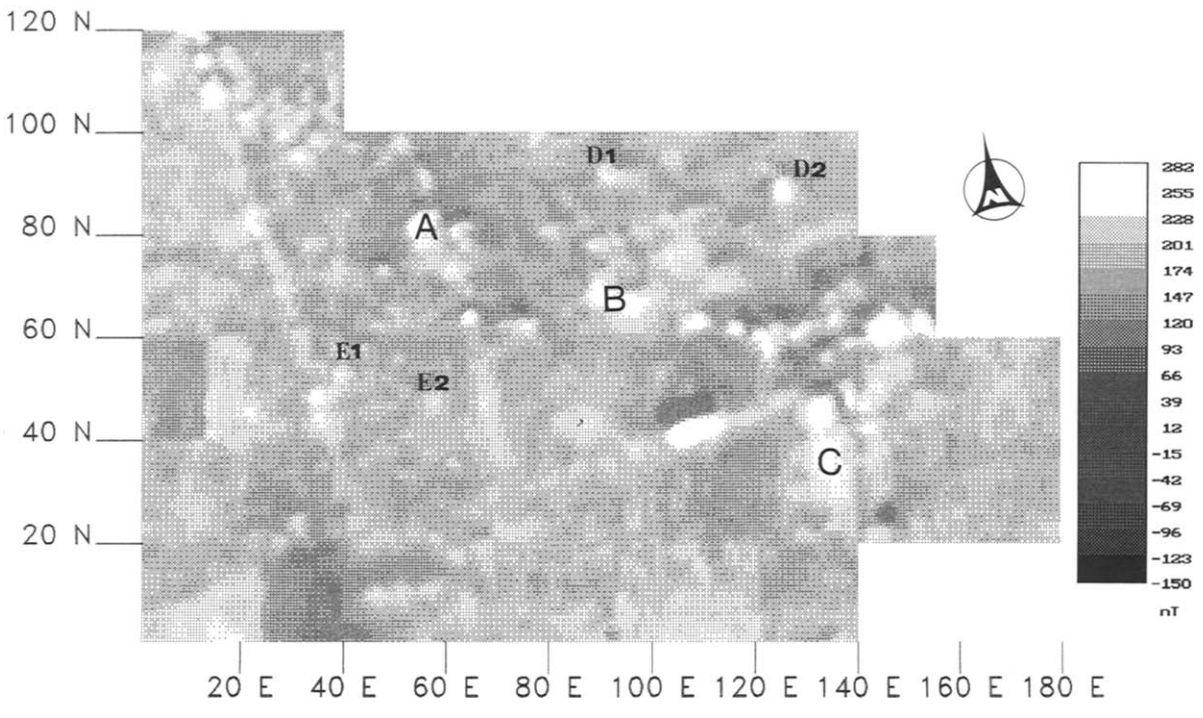

Fig. 3. Grey scale image of the magnetic data of the Acropolis (*AKR*). It corresponds to squares 1–42 of Fig. 2 which are outlined there by a bold line. The values of the magnetic field strength which were encountered are in the range −150.4 to 286.5 nT; that range was divided in 16 equal portions which are depicted in the image as grey tones. These tones are displayed in reverse mode, i.e. the white represents the highest values encountered and the black the lowest. The letters *A*, *B* and *C* mark the locations of high positive anomalies attributed to the presence of buried relics belonging to large structures. In particular the anomaly annotated as *C* is due to a "destruction phase" created after the collapse of a large building. Anomalies annotated as *D*1 and *D*2 and several others of the same attitude are attributed to kilns. Anomalies marked with *E*1 and *E*2 are examples of anomalies caused by fire hearths.

tions. The first one is to remove anomalies which have a spiky appearance and are caused by near surface metallic hazard. The second one consists in filling up gaps in the data set. Both these cases were treated simultaneously. The gaps in the data, either due to data missing or, to the removal of a spiky, anomaly, were replaced by field values produced by interpolation from the surrounding area. Thanks to the almost perfectly levelled survey area and to the absence of excavation pits in it, we had no gaps larger than two grid units. Therefore, simple linear interpolation was used. Smoothing was performed by convolving the data set with a Hanning operator of the form:

0.06	0.10	0.06
0.10	0.36	0.10
0.06	0.10	0.06

The data were then transformed into an image. The definition of "image" is of a 2-dimensional matrix with elements representing the strength of the field in equally spaced points. The matrix can be displayed on a computer monitor if the strength is depicted as brightness of the respective pixels which now represent the elements. However, the geophysical data almost never appears in large numbers which could be shown in an one to one correspondence with the pixels of a high-resolution display. Therefore, the original data matrix has to be enlarged to fit such a requirement imposed by hardware. Enlargement of the data matrix is essentially an interpolation process whereby many output pixels are generated from fewer input values (Scollar et al., 1986). In our case, the technique of bicubic spline interpolation was used.

The residual magnetic field values vary from −150.4 to 286.5 nT having a standard deviation of 21.22 and a zero mean. That dynamic range of the data was divided into 16 bands which were depicted as 16 brightness levels giving thus "a grey scale image of 16 tones". Several strong anomalies of limited areal extent can be observed on that figure. They were attributed to the presence of kilns, fire hearths and "destruction phases" at the particular locations. A "destruction phase" is what is created after the collapse of a roof, i.e. a mesh of bricks, tiles, disintegrated wood and nails. They are usually simulated by a magnetic horizontal slab. However, the most striking features of the image are the long linear anomalies which reflect possibly the main streets of the ancient city.

The positive anomalies, marked as *A*, *B* and *C*, show a considerable areal extent. They were attributed to the remains of large structures which could be temples, administrative buildings, odeon or theatre (Fig. 3).

Apparent susceptibility measurements were carried out on samples of various materials found in the Acropolis as well as on samples of the top-soil and sub-soil layers. The average values observed are as follows:

(1) Hewn stones (limestone)	8.760×10^{-5}
(2) Tiles (clay)	1.687×10^{-2}
(3) Bricks (clay)	2.121×10^{-3}
(4) Topsoil (<40 cm depth)	5.234×10^{-4}
(5) Subsoil (>40 cm depth)	2.480×10^{-4}

2.2 Resistivity prospecting

Resistivity prospecting took place in the same location and covered the shaded area which is crossed by E–W ranging lines area in Fig. 2. The area is also outlined by a dashed bold line in the same figure. The "twin probe" array (Aspinall and Lynam, 1970) was employed, which is often called a "split dipole array". A current electrode and the corresponding potential one (say $C-$ and $P-$) are placed in a remote area and the other current and potential electrode (say $C+$ and $P+$) are transported from each measuring position to another. The mobile probes are fixed rigidly in a wooden frame and therefore a compact system, convenient for rapid surveying is formed. In fact, only one operator is enough for such a system since the particular

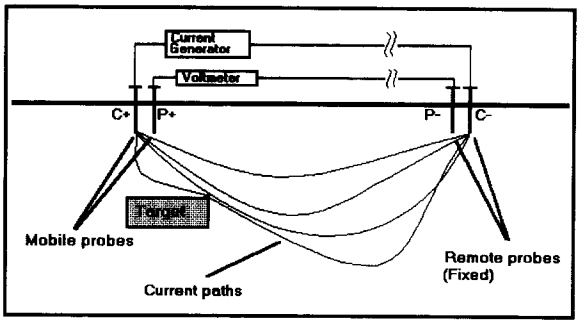

Fig. 4. Sketch diagram of the "twin probe" or "split dipole" array. In the case of Akropolis the spacing of the roving electrodes was 0.5 m while in the case of the cemetery it was 1 m.

instrument which was used had an internal solid state memory capable of storing thousands of readings. The remote (stable) electrodes have to be away from the nearest measuring point at least 30 times the spacing of the mobile ones (Fig. 4). In this case it can be easily proved (Aspinall and Lynam, 1970) that the configuration factor of the array is approximately $\pi\times a$ where a is the spacing of the mobile probes. A spacing of 0.5 m was used for the search in the Akropolis.

The system is capable of swift operation. For instance, approximately 45 min were needed to measure a 20×20 m^2 square in our case. Measurements were carried out along the same mode as the magnetic ones, i.e. with 1 m grid unit, employing the RM15 instrument of the *GEOSCAN RESEARCH*, and the data were transformed into an image in the same way as the magnetic ones.

Although the weather during the survey was fairly constant, the background level of the measurements varied for different days due to variation of the moisture content in the topsoil. In order to suppress these discrepancies between the various 20×20 m^2 squares, the background level was equalized for all of them. This was succeeded by adding the appropriate factor to the measurements of each square. The results are shown in Fig. 5 as an image consisting of 16 grey levels. It is easily observed that the urban network of the latest phases is revealed because the ruins of the foundations are shown clearly in the images. They are expressed by the dark alignments which presumably reflect the high resistivities encountered. The existence of two different directions in the ancient building activity suggests the presence of two distinct historical phases whose ruins

Fig. 5. Grey scale image of the spatial distribution of apparent resistivities encountered in the surveyed area at the Acropolis. Data has been smoothed and the level has been equalized adding an appropriate factor to each measured square. The image consists of 16 grey levels which reflect equal portions of a dynamic range of 35 to 157 Ohm·m. The urban network shows two distinct building directions which presumably correspond to different habitation phases. The building directions which revealed by the excavation carried out in the pit drawn in the figure, correspond perfectly with the geophysical image. This pit is located in the southwest corner of the image.

are close to the ground surface. This is also obvious in Fig. 6 where all the resistivity data are shown in dot density mode in order to give them another more "blocky" appearance (Scollar et al., 1986). In this technique, a number of dots is plotted in a small area around each measuring position. The number is analogous to the field strength at each position. The result resembles the stippled drawings often used to record the excavation results.

The main roads of the urban complex are also evident in Fig. 6 and their locations have been annotated as *A* and *B*. Indeed, the letters *A* and *D* mark the locations which have been enlarged and are shown in Fig. 7. In particular the wall complex, illustrated in the lower part of Fig. 7, seems to belong in a different phase than that of the system of main roads which produced the pronounced magnetic anomalies. Nevertheless, the details of the whole image which have been plotted in Fig. 7

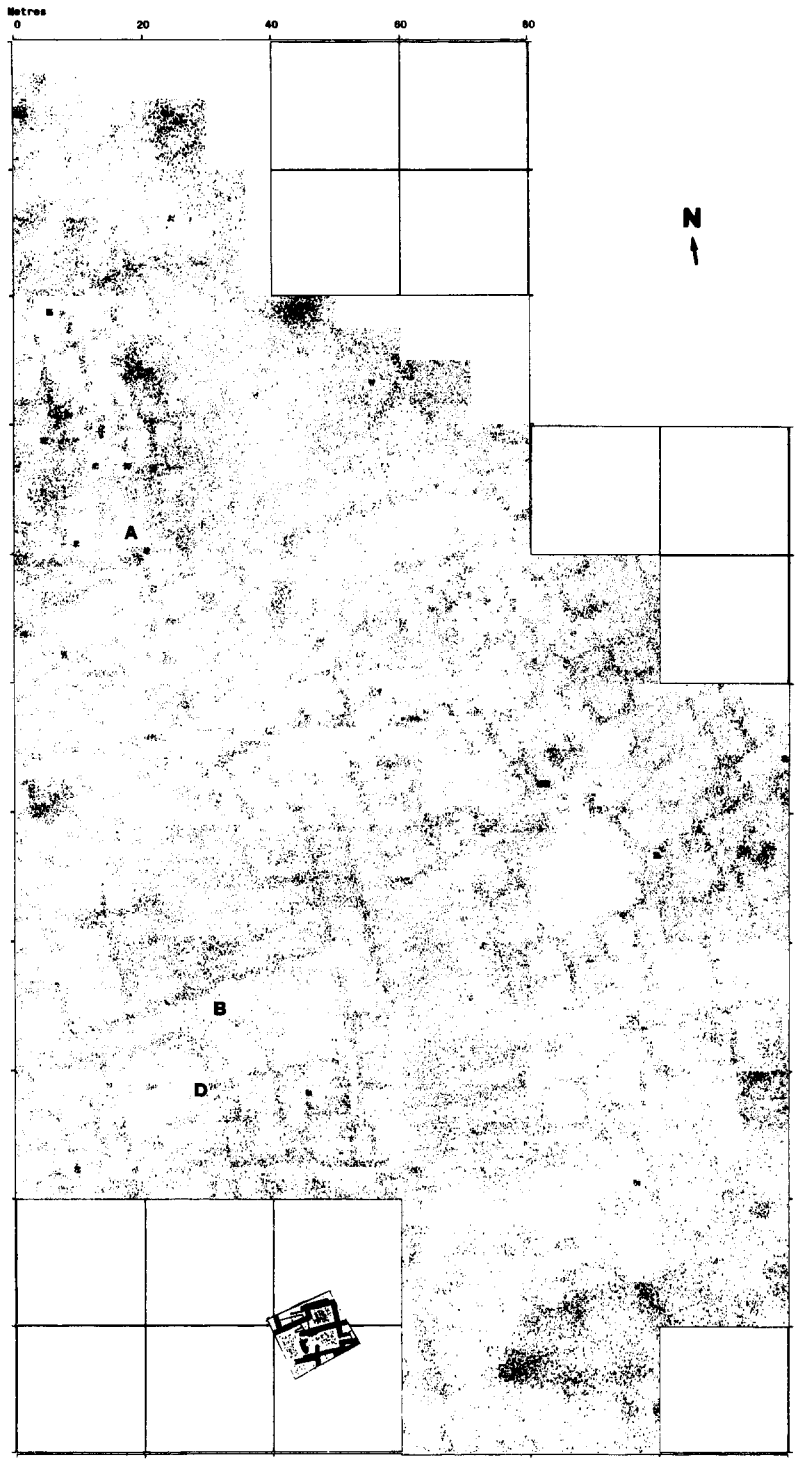

Fig. 6. Spatial distribution of apparent resistivity in the area of Acropolis covering the same locations as those of Fig. 5 plotted in dot density mode. The excavation along with its findings is also drawn for comparisons.

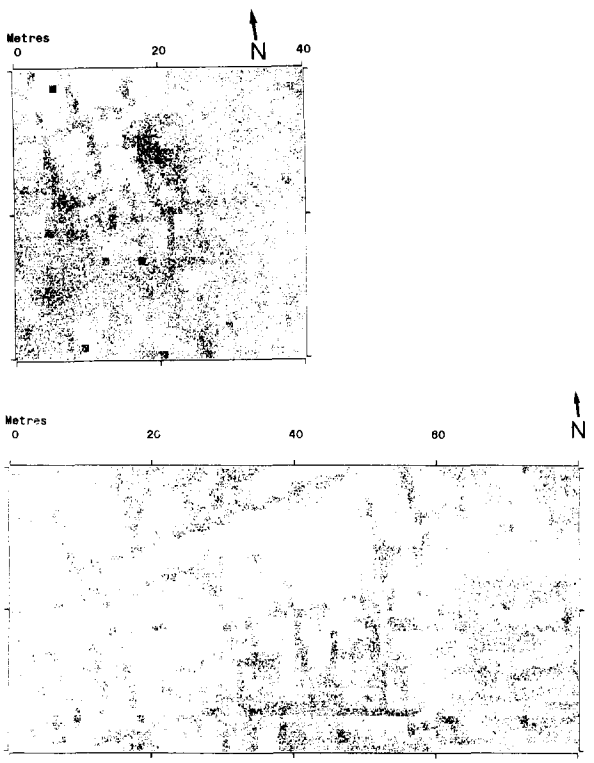

Fig. 7. Details of the result of the resistivity survey in the Acropolis. The locations marked as *A* and *D* in Fig. 6 are presented in the upper and lower part, respectively. The buried ruins that express themselves in the geophysical images belong to the foundations of once existing buildings.

show clearly the foundations of the once existing structures as well as parts of the system of roads once crossing the city.

The magnetic image of Fig. 3 and the electrical one of Fig. 5 must be seen as complementary one to the other. Although the electrical one is more impressive, some additional information about structures affected by fire is given in the magnetic image. Taking into account both images and the susceptibility measurements, one can conclude that the long alignments of the magnetic image reflect definitely the main streets of the city. They express themselves as positive anomalies mainly because bricks and tiles from buildings which stood alongside have filled up the paths. Another reason, but of secondary importance, is that they have been filled up with topsoil also which is slightly more magnetic than the subsoil.

3. Search in the area of workshops

The area marked with the code *EUP* in Fig. 2 is situated at the foothills of the Acropolis. This is presumably the area where the workshops of various craftsmen should have been located. This results from the fact that this location is outside the wall protected area on the gently sloping side of the hill while the slope is steep in any other side. Consequently, one could approach the Acropolis from this side only, where the main road leading to the city should have been built. Alongside that road was presumably the best location for the workshops.

The area was prospected employing the magnetic field gradient method. The instrument used was a differential fluxgate magnetometer of the *GEOSCAN RESEARCH*. Measurements were taken in the same fashion as in the case of Acropolis and transformed into an image along the same baselines. After smoothing the gradient values varied from −45.7 to 74.7 nT/m having a zero mean and a standard deviation of 3.15. The range was divided by 16 levels and the resulting image is shown in Fig. 8A. Several anomalies that can be attributed to kilns and fire hearths are shown. The most pronounced is the one which is located at the southwestern corner of the image. The anomaly is caused by a feature possessing strong positive susceptibility contrast against the hosting medium since its amplitude exceeds 120 nT/m (before smoothing with the Hanning operator). The trial pit which was dug in the particular spot is drawn in any relevant figure and the finding itself is illustrated in Fig. 8B (a well preserved pottery kiln of the Hellenistic era).

The circular anomalies present in Fig. 8A probably reflect the existence of trenches which were opened in relatively later times. Other features are also present which could be attributed to ruins of buildings.

4. Resistance and GPR surveying for monumental tombs

The locations annotated as *EURCEM* and *EURES* in Fig. 2, cover the place used as cemetery during the

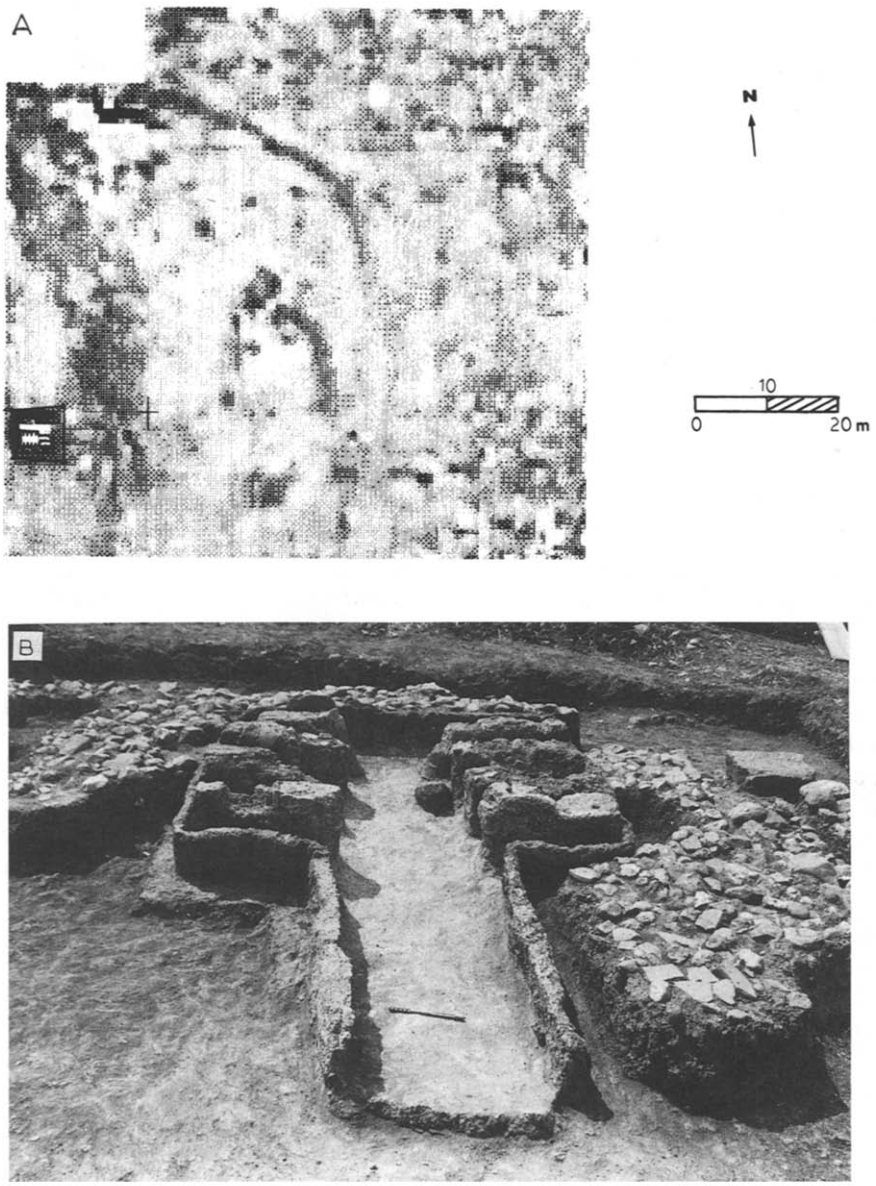

Fig. 8 (A) Distribution of the magnetic total field differential values in the area covering the foothills of the Acropolis and comprising the place of the ancient workshops. The data are presented as a grey scale image consisting of 16 tones in reverse mode. The pronounced anomaly in the southwestern corner is due to the kiln shown in (B) which was revealed after excavation. That kiln was buried in about 0.4 m depth and is also shown in plane view along with the magnetic image.

Roman era. It was prospected using the "twin probe" array with a spacing of 1 m for the mobile probes and employing an *ABEM TERRAMETER*. The objective was to locate the monumental tombs concealed in the area and selectively guide the excavations. In archaeological terms, the tombs that have not been looted are very important findings since the ancient Greeks used to put valuable artifacts there because of their funeral beliefs. The targets were expected to be buried in less than 1 m deep clay cover which is conductive by any means. Their lateral dimensions expected to be of the order of a few meters. Of course, they should have been constructed using stone blocks and bricks and thus being resistive even if they had collapsed.

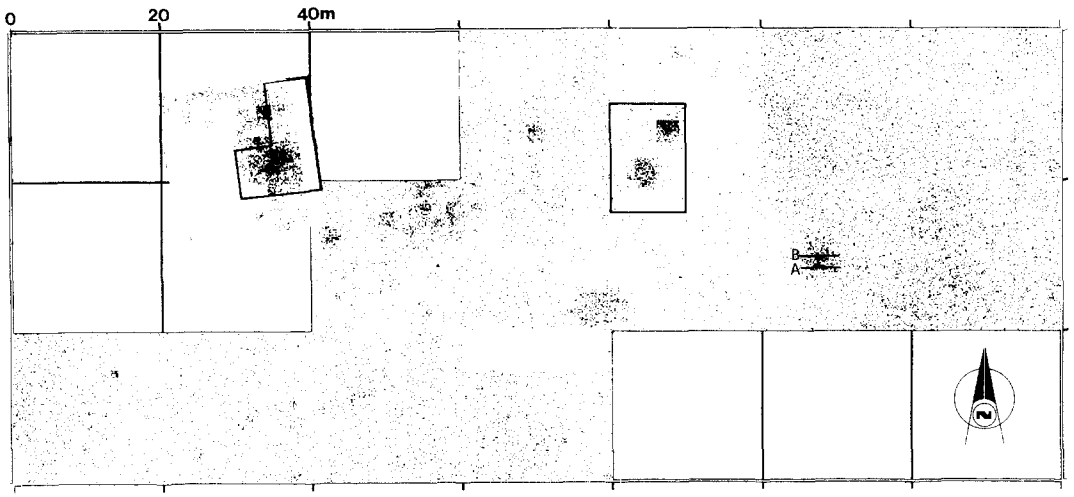

Fig. 9. Dot-density plot of the spatial distribution of the resistivity in the area of a cemetery of the Roman era belonging to the ancient city of Europos, values range between 20 and 150 Ohm·m. Anomalies due to large resistive features are attributed to concealed monumental tombs. The edges of the pits dug after the survey was completed are also drawn in the picture. The letters *A* and *B* mark the traces of GPR profiles carried out.

The results are shown in Fig. 9 in the form of a dot-density plot of the distribution of apparent resistivity. The locations of the excavation pits are also shown and the respective findings are presented in Fig. 10. From the geophysical point of view, several experiments could be designed since the location of unearthed large tombs is precisely known. In other words, the area could be used as a natural laboratory where targets exist in a relatively homogeneous environment. However, from the archaeological point of view, the excavation of those tombs has been postponed till the necessary financial means become available. On the other hand, information concerning their number, their attitude (e.g. monumental) and their positioning in space is not lost and can be used in any historical evaluation about the area.

Having in mind the relatively high resolving ability of the GPR method we conducted several profiles crossing the structures producing the pronounced resistivity anomalies. The *ERA TECHNOLOGY* GPR system of the carrier-free type was used for this purpose. The system emits pulses of 1 or 2 ns duration and its antennae bandwidth is 200 Mhz to 2 Ghz. That system employs linearly polarized resistively loaded dipoles for its transmitting and receiving antennae. Daniels et al. (1988) showed that this type of antenna has low radiation efficiency. On the contrary, its small physical size and polarization state were counted as significant advantages by the same researchers. With respect to the polarization state, we used the crossed antennae configuration, i.e. the transmitting and receiving one were orthogonal each to the other. The cross configuration results in a reduction to the coupling effect between the antennae. Also it is insensitive in planar targets and therefore in the air–earth interface (Chan et al., 1979). On the contrary, the air–earth interface is shown as a strong reflection if the parallel antennae configuration is used and one has to remove it by muting. Transmission and reception took place at the same physical location, i.e. a zero-offset survey was performed.

The record length was fixed to the 51.2 ns using a sampling interval of 200 ps. Therefore, each record consisted of 256 data points. A 64-fold stacking was used in order to enhance the signal to noise ratio. The system's clutter was reduced by subtracting the mean waveform. Such an operation can be carried out by assuming that the energy scattered backwards by the targets is spread in a few waveforms only close to the zero offset one.

To compensate for the attenuation of the signal due to the lossy medium of propagation, an exponential gain was applied to the data. This operation gives optimum results only if the attenuation constant and the velocity of propagation are known. Usually only estimates of these values are available and the success of

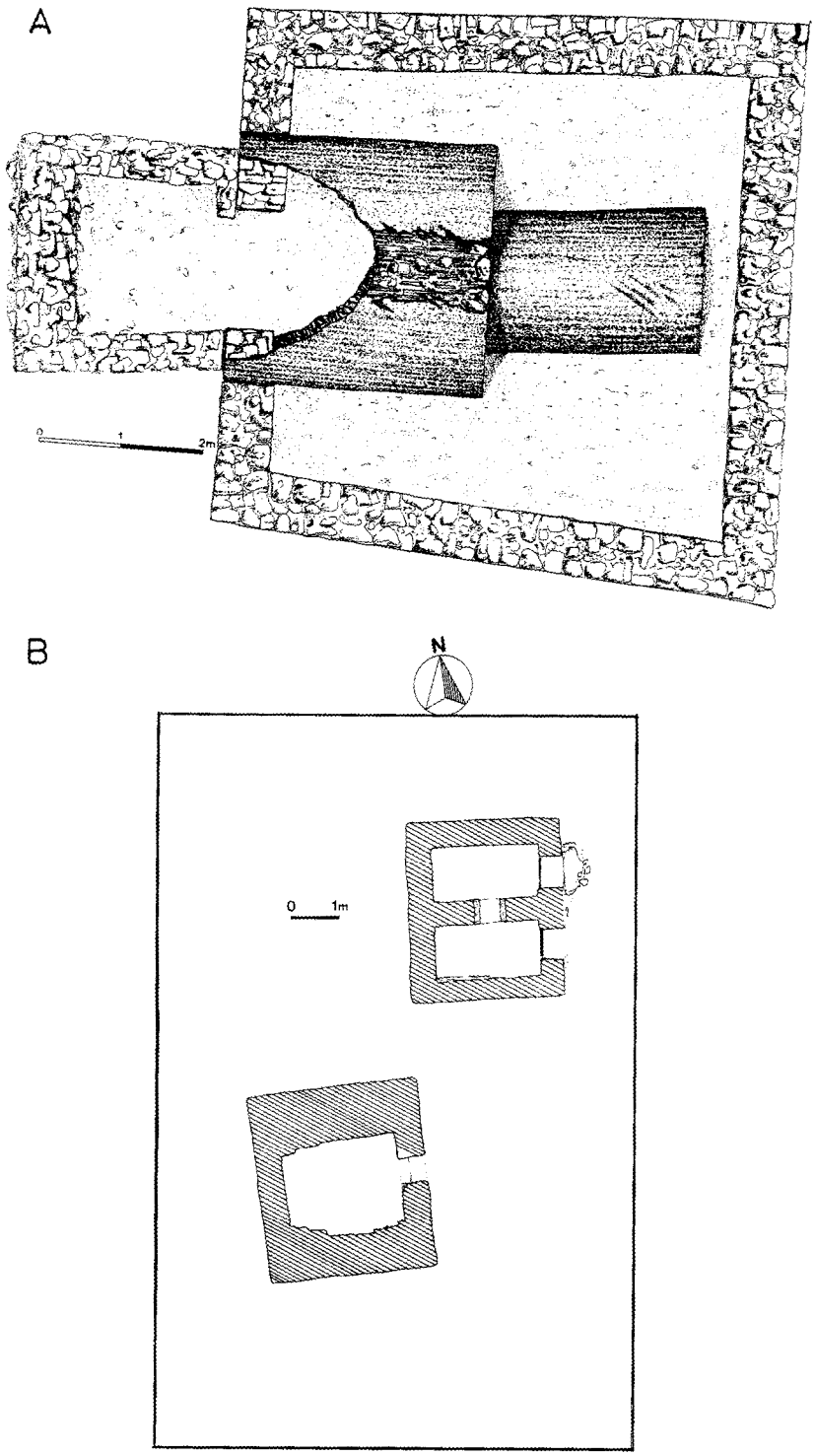

Fig. 10. (A) Plane view of the monumental tomb causing the pronounced anomaly in the square which is the only oblique one relatively to the others. The well posed pair of anomalies in Fig. 9 was caused by the pair of tombs shown in (B). The tombs were buried at 0.5 m depth and were constructed partly by hewn stones and partly by bricks. Both roofs of the pair of tombs had been collapsed and they had been filled with clay material. Their lateral dimensions are of the order of 3×4 m and their vertical one was about 2.5 m.

the gain procedure is mostly dependant on the operator's expertise. The gain function which was implemented to our processing module is:

$$W_i^{\text{gained}} = W_i^{\text{old}}\, e^{\alpha c i \Delta t / 8.69 \sqrt{\epsilon'}}$$

where α is the attenuation in db/m, c the velocity of light in free space, Δt is the sampling rate, i the index of the data points, and ϵ' the real part of the assumed complex relative permittivity of the medium (Moffat and Puskar, 1976).

Our objective was to gain some more information about the tombs and mainly to conclude if their arch roof was still standing or had collapsed. In the second case, it is more likely that the tomb has been looted and therefore it possessed minor archaeological interest. This is the case of the twin tombs shown in Fig. 10 where their walls are in good condition while their roofs have been destroyed.

A large number of GPR profiles were measured throughout the cemetery area. Two typical cases were

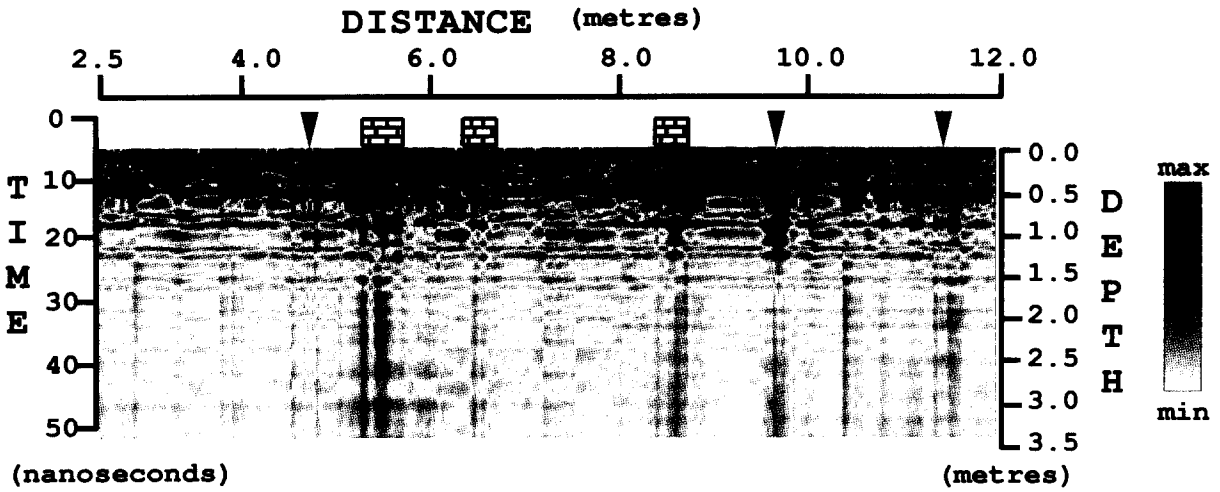

Fig. 11. GPR time section along profile *A* of Fig. 9 plotted in grey scale mode. The locations where reflections occurred which were attributed to the walls of a monumental tomb are marked with proper simulation. The arrows mark the locations where back scattered energy indicates the presence of buried walls or small tombs.

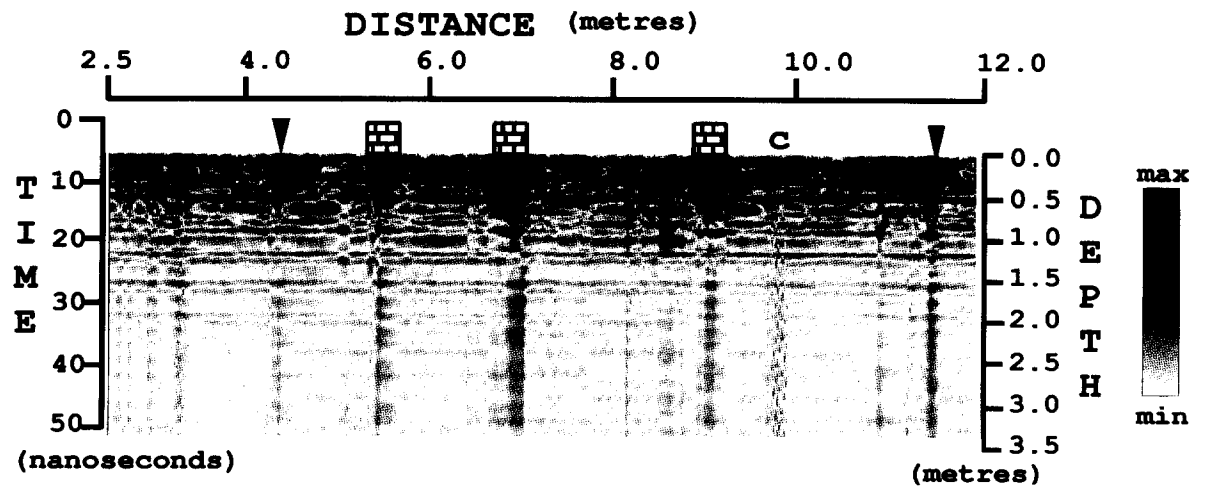

Fig. 12. GPR time section along profile *B* of Fig. 9 plotted in grey scale mode. Annotations are the same as in Fig. 11. The letter *C* denotes the part of the section where clutter appears. This was attributed to perturbations of the antennae cart on the rough terrain.

selected for presentation in these pages. Figs. 11 and 12 show the time sections obtained by the profiles annotated as *A* and *B*, respectively, in Fig. 9. Strong reflections with their multiples are observed, corresponding to the presence of walls belonging to a monument. Sketch drawings of walls mark the respective locations. The interpretation of the GPR data clearly shows the presence of a monument consisting of two compartments. This is very common in the area. Also, some other resistive features give well posed reflections which are marked by thin arrows. These are caused either by small tombs, scarce among the monumental ones or some of them might be enclosure walls like those of the monument shown in Fig. 10A. The tomb seems to be roofless otherwise a strong reflection would had been observed. In other words, the GPR data added some more information about the structure spotted by the resistivity prospecting.

However, the GPR operation requires a lot of power consumption, storage media and processing time to explore the area in the same sense as the resistivity prospecting. Also, due to the nature of the method, the results can not be presented in a form of images resembling the plane view drawings of the excavation results. This means that the GPR method is a rather inconvenient one for large scale exploration.

The rough terrain brings some noise to the system which is the case marked as *C* in Fig. 12. This case is rather pronounced but always a small amount of clutter will be fed into the system if operated in open fields since no perfectly levelled fields can be found. It seems that clutter can be reduced considerably if the antennae are moving on a flat surface. Therefore, it can be used within standing monuments searching for cavities for instance. In that case the method should reach its maximum performance since the dielectric constants are expected to be low. Nevertheless, the GPR method is a powerful one in resolving ability due to the small wavelengths used. This is well illustrated in the examples presented here.

In order to estimate the GPR's penetration depth and also to convert the time axis of the GPR image to depth, an estimation of the attenuation and of the propagation velocity of the medium is needed. The propagation velocity is calculated using the relation:

$$V=\frac{c}{\sqrt{\epsilon'}}$$

In this case, the real part of the relative permittivity of the medium, ϵ', is assumed as constant over the GPR's frequency range (Davis and Annan, 1989). For a dry clay soil, as in the surveyed area, the value of 5 (Campbell, 1992) was assumed for ϵ'. Consequently, a velocity of propagation of 0.15 m/ns was estimated. However, one should bear in mind when transforming the time axis to a depth, the two way travel path of the signal.

The penetration depth is calculated from an estimation of the attenuation in the medium of propagation. However, a carrier-free system emits pulses of electromagnetic energy which have a wide frequency spectrum. Therefore, the linear dependence of the attenuation with frequency (Daniels, 1977; Turner, 1992) has as a consequence the broadening of the pulse with depth due to the stronger attenuation of its high-frequency components (Vainkainen et al., 1992).

In this study, we used the 250 Mhz frequency so as to determine approximately the greatest penetration depth. For the type of soil we mentioned above and that particular frequency we adopted an attenuation of 0.8 db/m (Olver et al., 1982). Therefore, for a 3 db reduction of the signal amplitude the penetration depth is 1.87 m having in mind the two way travel path. One should notice that no signal is registered after about 25 ns. This means that this time limit corresponds approximately to the previously estimated depth.

5. Conclusions

The case history presented in these pages comprise a large scale geophysical exploration of an archaeological site. The survey was aiming at various targets and therefore several methods and settings were employed. The result was that it led to significant archaeological findings. The foundations of the buildings of the main urban complex have been revealed and depicted in a manner compared to a drawing of an excavation results. As a secondary consequence, several conclusions were drawn regarding the location of public buildings. These locations are the most important targets for selective excavation. Features like destruction phases, hearths and kilns were also spotted out by magnetic prospecting. A pottery kiln was revealed at the foothills of the former area, and several other kilns were also spotted in the same area.

Three monumental structures used as tombs were discovered and unearthed by electrical prospecting in the area of a cemetery. The location and the approximate dimensions of several others were also revealed. However, the main impact of geophysical prospecting is that the relevant archaeological and historical conclusions can be obtained without extensive excavation in an inexpensive, swift and non-destructive manner. The digging can also be directed selectively. The Ground Probing Radar is very useful in resolving targets identified by other methods.

Acknowledgements

The whole survey in the archaeological site of Europos was financed by the Greek Secretariat of Research and Technology. Also, the authors are indebted to Prof. B.C. Papazachos for his careful reading of the manuscript and his useful suggestions.

References

Aspinall, A. and Lynam, J.T., 1970. An induced polarization instrument for the detection of near surface features. Prospez. Archaeol., 5: 67–75.

Astaras, T.A. and Sotiriadis, L., 1988. The evolution of the Thessaloniki–Gianitsa plain in Northern Greece during the last 2500 years—from Alexander the Great until today. Proc. INQUA/IGCP Meet. Palaeohydrological Changes during the last 15000 years, Bern, June 1985. Balkema, Rotterdam, pp. 105–114.

Campbell, T., 1992. A Structured Evaluation of Ground Penetrating Radar for Archaeological Use. M.Sc. thesis. Univ. York, 150 pp.

Chan, L.C., Moffatt, D.L. and Peters, L.J.R., 1979. A characterization of subsurface radar targets. Proc. IEEE, 67(7): 991–1000.

Daniels, D.J., 1977. The Use of Radar in Geophysical Prospecting. RADAR-77, IEE Conf. Publ., 155, pp. 540–546.

Daniels, D.J., Gunton, D.J. and Scott, H.F., 1988. Introduction to Subsurface Radar. IEE Proc., 135, F, 4, pp. 278–320.

Davis, J.L. and Annan, A.P., 1989. Ground-penetrating radar for high-resolution mapping of soil and rock stratigraphy. Geophys. Prospect., 37: 531–551.

Moffat, D.L. and Puskar, R.J., 1976. A subsurface electromagnetic pulse radar. Geophysics, 41(3): 506–518.

Olver, A.D., Cuthbert, L.G., Nikolaides, M. and Carr, A.G., 1982. Portable FMCW radar for locating buried pipes. RADAR-82, IEE Conf. Publ., 26, pp. 413–418.

Sarris, A., 1992. Shallow depth geophysical investigation through the application of magnetic and electric resistance techniques. Ph.D. thesis. Univ. Nebraska, Lincoln, NE, pp. 597 pp.

Scollar, I., Weidner, B. and Segeth, K., 1986. Display of archaeological magnetic data. Geophysics, 51(3): 623–633.

Turner, G., 1992. Pulse distortion due to reflection in ground penetrating radar surveying. 54th EAEG Meet., Paris, pp. 462–463.

Vainikainen, P., Tiuri, M., Kontra, V. and Nyfors, E., 1992. Portable short range subsurface radar. 4th Int. Conf. Ground Penetrating Radar, Rovaniemi, Spec. Pap., 16, pp. 29–33.

Weymouth, J.W. and Lessard, Y.A., 1986. Simulation studies of diurnal corrections for magnetic prospection. Prospez. Archaeol., 10: 37–47.

Wynn, J.C., 1986. Archaeological prospection: An introduction to the special issue. Geophysics, 51(3): 533–537.